EINDHOVEN
UNIVERSITY OF
TECHNOLOGY

Characterization method for mechanical properties of thin freestanding metal films for RF-MEMS

Citation for published version (APA):
Burg, V., Toonder, den, J. M. J., Dijken, van, A., Hoefnagels, J. P. M., & Geers, M. G. D. (2006). Characterization method for mechanical properties of thin freestanding metal films for RF-MEMS. In *Proceedings of EuroSimE 2006* (pp. 24-30). Institute of Electrical and Electronics Engineers.

Document status and date:
Published: 01/01/2006

Document Version:
Accepted manuscript including changes made at the peer-review stage

Please check the document version of this publication:

• A submitted manuscript is the version of the article upon submission and before peer-review. There can be important differences between the submitted version and the official published version of record. People interested in the research are advised to contact the author for the final version of the publication, or visit the DOI to the publisher's website.
• The final author version and the galley proof are versions of the publication after peer review.
• The final published version features the final layout of the paper including the volume, issue and page numbers.

Link to publication

General rights
Copyright and moral rights for the publications made accessible in the public portal are retained by the authors and/or other copyright owners and it is a condition of accessing publications that users recognise and abide by the legal requirements associated with these rights.

• Users may download and print one copy of any publication from the public portal for the purpose of private study or research.
• You may not further distribute the material or use it for any profit-making activity or commercial gain
• You may freely distribute the URL identifying the publication in the public portal.

If the publication is distributed under the terms of Article 25fa of the Dutch Copyright Act, indicated by the “Taverne” license above, please follow below link for the End User Agreement:

www.tue.nl/taverne

Take down policy
If you believe that this document breaches copyright please contact us at:

openaccess@tue.nl

providing details and we will investigate your claim.

Download date: 08. Dec. 2024

Characterization Method for Mechanical Properties of Thin Freestanding Metal Films for RF-MEMS

Vincent Burg[1,2], Jaap den Toonder[1,2], Auke van Dijken[1], Johan Hoefnagels[2], Marc Geers[2]
[1] Philips Research Laboratories Eindhoven, The Netherlands
[2] Eindhoven University of Technology, The Netherlands

Abstract

A method for the characterization of mechanical properties of freestanding thin metal film materials used in RF-MEMS is evaluated. Freestanding beam structures are manufactured from a sputtered layer of AlCu(1wt%) on top of a wafer using an industrialized RF-MEMS manufacturing process. The methods of examining microstructure and geometry are studied. It is shown that these methods are promising for extracting the desired information about the material. Simple bending experiments are carried out on micro-scale beams of varying length and thickness using an indenter device. Elastic material properties are extracted from the results, using finite element technology combined with elastic theory, removing the necessity of extensive finite element simulations. It is shown that the beam length and indenter positioning play a crucial role. The obtained results show agreement with expected values for longer beams, but no obvious relation with the film thickness is found within the experimental range addressed.

1. Introduction

Application

At the current pace of technology the demand for smaller devices with higher performance is increasing. RF-MEMS are likely to play an important role. RF-MEMS are micro-electromechanical systems (MEMS) with applications in wireless RF (radio frequency) communication devices such as mobile phones. Size considerations will require the integration of components in a single chip. Compared to conventional p-i-n diodes, RF-MEMS show improvements in insertion loss, power consumption and isolation. Particular application functions that are being developed are filters, inductors, tuneable capacitors and switches.

RF-MEMS are either made from silicon (e.g. filters) or from thin metal film material (e.g. variable and switching capacitors). This study focuses on the thin metal film type. Figure 1 shows an RF-MEMS tuneable capacitor, which consists of a freestanding thin metal film (thickness typically 5 μm) suspended over an air gap, which is varied to change the capacitance ratio. RF-MEMS are made using standard IC processing techniques like PASSI™ technology, a patented passive integration manufacturing process by Royal Philips Electronics N.V. [1], which uses aluminium alloys to create RF-MEMS. This technique creates the possibility to integrate the devices with other components on a single chip.

Permanent Deformation

Permanent deformation can be introduced during manufacturing as well as during use of the devices. This is obviously unwanted to ensure the required reliability. Permanent deformation in metals, such as used in these devices, is generally caused by either plasticity or creep.

Plasticity originates from the movement of dislocations in crystal grains in the material when the yield stress is exceeded. During manufacturing a number of heating steps are taken in which the devices are kept at high temperatures (up to 200˚C) for a significant amount of time (up to 45 minutes), which can cause stresses above the yield stress due to thermal expansion. Figure 2 shows a SEM picture of an RF-MEMS tuneable capacitor, which is permanently deformed due to stresses during manufacturing.

Creep also involves the movement of dislocations, but occurs below the yield stress when the stress is maintained for a period of time. This phenomenon might occur during the use of the device when a certain stress

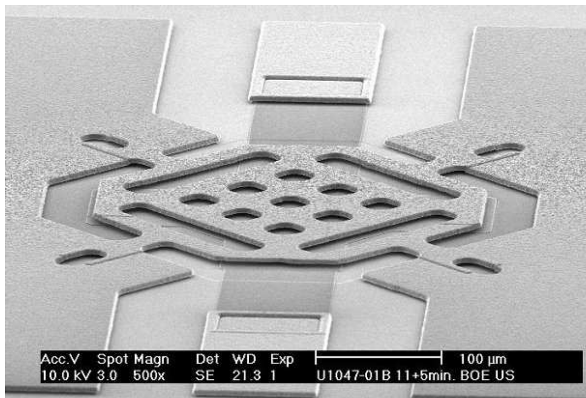

Figure 1: RF-MEMS tuneable capacitor

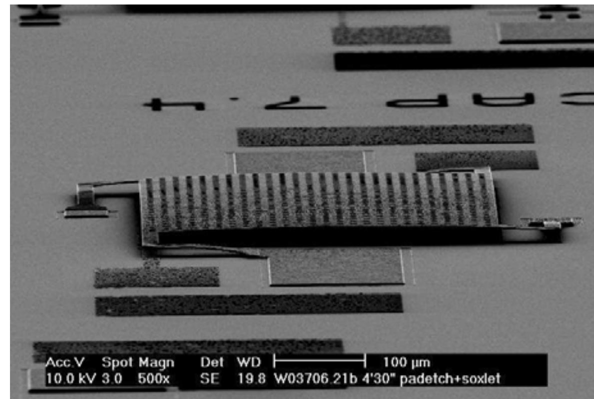

Figure 2: Permanent deformation caused by manufacturing process

Authorized licensed use limited to: IEEE Xplore. Downloaded on December 11, 2008 at 01:15 from IEEE Xplore. Restrictions apply.

state is held for a longer period. Creep effects are not studied in this work.

Thin Film Mechanics

The properties of a material are generally determined by the interaction or competition of a characteristic internal length scale, e.g. spacing between dislocations, with a microstructural size parameter, e.g. grain size [2]. When these length scales approach each other classical relations break down. In thin films this is the case because the grain diameter is generally of the same size or larger than the film thickness and thus the material behaviour cannot simply be scaled down from the bulk behaviour.

The movement of dislocations is heavily influenced by geometric boundaries in grains, including the external boundaries of the film. Since different types of boundaries have a different effect on dislocation movement, this also influences permanent deformation mechanisms.

When dislocations pile up along boundaries, repulsing stresses develop, slowing down the movement of incoming dislocations. This might be the case at a grain boundary or the boundary between a grain and a precipitate. By slowing down dislocation movement the material is resisting permanent deformation, thus explaining the strengthening effects of grain refinement and precipitation hardening.

At free boundaries, e.g. at the edge of the geometry, dislocations are allowed to move out of the material by slip between crystallographic planes, leaving behind a surface step. These types of boundaries have no induced stress fields and do not prevent other dislocations from gliding towards the boundary. This allows more permanent deformation, effectively weakening the material.

Freestanding thin metal films exhibit behaviour very different from bulk material as found in previous studies. Especially the yield stress turns out to be much lower for freestanding thin films compared to bulk material, while a sharp increase can be seen with thin films on a substrate [3]. Freestanding thin metal films have a small number of grains in the thickness direction and therefore a large free area compared to bulk material. Taking the above-mentioned phenomena into account, the difference in material behaviour can be explained qualitatively.

Objective

The goal of this study is to investigate a particular experimental method to determine the mechanical properties of freestanding thin metal film used in RF-MEMS. The investigated method can be used to investigate the size effects in the material properties. The following strategy will be evaluated:

- Freestanding test structures of varying geometry and thickness are designed and manufactured using an existing manufacturing process for RF-MEMS.

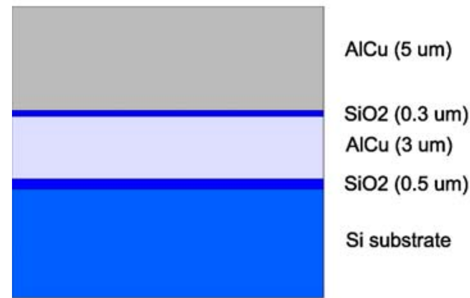

Figure 4: Initial wafer stack

- The microstructure and the geometry of the sample material are investigated using several microscopic techniques.
- Bending experiments are carried out on the test specimens and the results are used to extract the mechanical properties.

2. Experiments & Methods

Sample manufacturing

The material used is AlCu(1wt%), a very promising material for RF-MEMS. Materials for RF-MEMS need to have good electrical properties i.e. high conductivity, as well as good mechanical properties.

The resulting stack consists of two metal layers and two silicon oxide (SiO_2) layers as shown in Figure 4. The two SiO_2 layers are used for electrical insulation and the lower metal layer is the sacrificial layer, which is removed under the sample beams to create the freestanding structure. The top metal layer is the AlCu(1wt%) layer which is investigated. The AlCu(1wt%) material is deposited on a wafer by sputtering for approximately 6 minutes, while temperatures rise up to 300˚C.

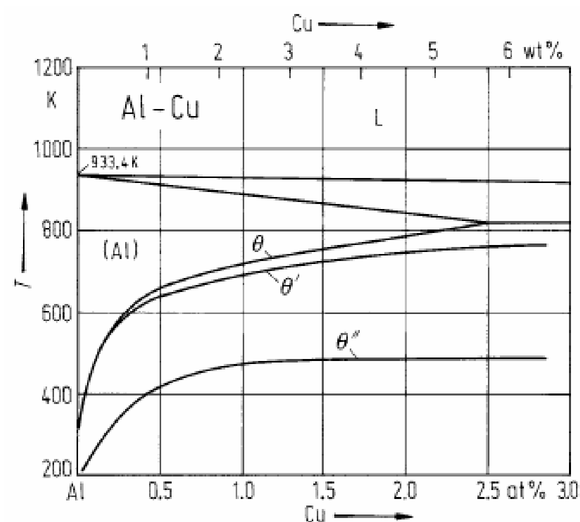

Figure 3: Al-Cu phase diagram (Al rich part) [4]

Authorized licensed use limited to: IEEE Xplore. Downloaded on December 11, 2008 at 01:15 from IEEE Xplore. Restrictions apply.

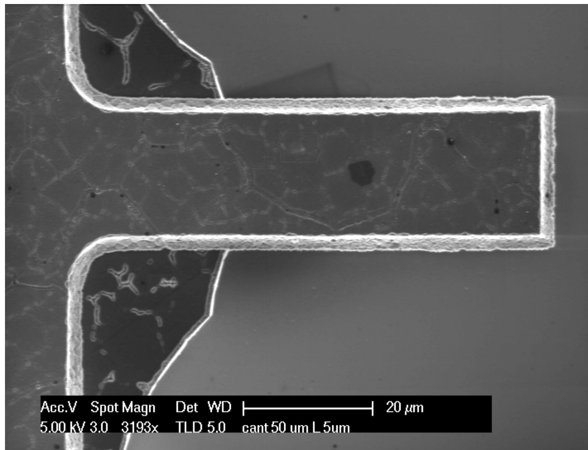

Figure 5: SEM micrograph of resulting beam structure

The phase diagram of Al-Cu shows the formation of three types of intermetallic phases (θ, θ', θ'', the latter two being intermediate phases) for AlCu(1wt%), as shown in Figure 3 [4]. When the cooling is slow enough to reach equilibrium state, only θ-phase particles will be formed, which are clusters of Al_2Cu in the α-phase (Al) crystal [5]. The formation of these θ particles, also known as precipitates, is the basis of precipitation hardening, a process which is dependent on the cooling speed.

Conventional wafer fabrication processing is used to create the micro-beams from the wafer stack. The process essentially consists of the application of a photosensitive resist, which is exposed through a mask with the desired pattern and developed to cure the desired parts. The cured pattern then protects the underlying material during the etching step and only this part remains present. This process is carried out twice, first to create the top metal structure and secondly to etch the sacrificial layer.

Cantilever structures are created having lengths ranging from 20 μm to 800 μm. The top layer thickness is initially 5 μm for each wafer and is reduced by an additional etching step in the beginning of the patterning process to create different layer thickness. The resulting wafers have a thickness of t_{des} = 3 μm, t_{des} = 4 μm and t_{des} = 5 μm by design, which need to be verified afterwards. Figure 5 shows a scanning electron microscopy (SEM) image of one of the resulting beam structures on the wafer.

Microstructure

The microstructure is investigated since its influence on the material properties will be significant, especially for thin films. Geometric boundaries, e.g. grain boundaries or precipitates, effectively strengthen a material. The relevant aspects of the microstructure are grain size in lateral and layer thickness direction, grain orientation and the composition, position and size of precipitates.

To investigate grain orientation and grain size orientation imaging microscopy (OIM) is used. This technique is an extension to an SEM, which analyses the diffraction patterns of back-scattered electrons (BSE) to retrieve crystal orientation information.

Table 1: MTS Nano Indenter XP accuracy [6]

Displacement resolution	<0.01 nm
Load resolution	50 nN
Contact force	<1.0 μN
Load frame stiffness	~1 x 10^7 N/m
Positioning accuracy	1.5 μm

Focused ion beam (FIB) is used to investigate the grain structure in thickness direction, which is especially interesting in thin metal film materials. FIB uses a focused beam of heavy ions (Ga+) to remove material from the specimen, allowing a view on the inside of the specimen.

Transmission electron microscopy (TEM) is used to find the position and size of the precipitates in the material. Energy-dispersive X-ray spectroscopy (EDX) is next used to determine the chemical composition of the precipitates.

Geometry

Due to the nature of the manufacturing process, the geometry of the specimens depends on etching speed and time, which are hard to predict and therefore the actual geometry somewhat deviates from the designed geometry, which requires verification measurements afterwards. The goal of the geometry measurements is to identify the specimen dimensions, revealing details on the actual predictability of the beam geometry.

The beam geometry is measured using a vertical scanning interferometer (VSI) microscope (Sensofar Plu2300), which creates a surface height map by analysing interference between reflected light from the sample and a mirror at a known distance. The lateral resolution of this device is 0.32 μm.

The geometric variation per wafer is studied first on the wafer with the largest thickness. These measurements are carried out on different beams, varying in beam length, orientation and location on the wafer.

Bending Experiments

The bending experiments are carried out by applying a force on the beams while recording displacement in time. The force is applied using a MTS Nano Indenter XP system, which also allows controlling the loading rate and hold time. The load is applied using a coil in a permanent magnet assembly, which is in a closed-loop feedback control system with a load sensor cell. The displacement of the indenter is measured using a three-parallel-plate capacitive position sensor. This set-up leads to the accuracies found in Table 1. The lateral positioning is done manually, using a crosshair on the screen, which leads to an additional positioning error of 1.5 um (half the pixel size in the used set-up) to be added to the system positioning error as reported by the manufacturer.

Authorized licensed use limited to: IEEE Xplore. Downloaded on December 11, 2008 at 01:15 from IEEE Xplore. Restrictions apply.

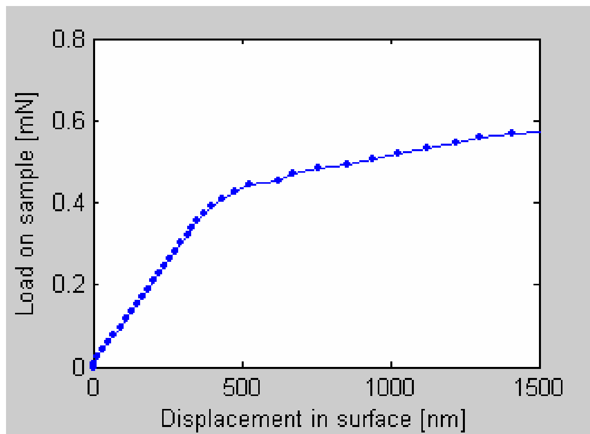

Figure 6: Example of measurement data as obtained from the Nano Indenter XP

The indenter used is a spherical indenter with a radius of 25 µm, which is chosen to reduce local deformation to a minimum, in order to measure pure beam deflection. The loading rate is chosen to be relatively fast (0.1 mN/s) to reduce the influence of creep effects.

Cantilever beams are used, which have the advantage that any present residual layer stress is relieved. For each designed thickness t_{des} = 3 µm, t_{des} = 4 µm and t_{des} = 5 µm, 3 designed lengths are tested: L_{des} = 30 µm, L_{des} = 40 µm and L_{des} = 50 µm. To study reproducibility 10 expected identical samples are sequentially tested. A typical load-displacement measurement result is shown in Figure 6**.** This figure shows the straight elastic segment of the curve and the plastic part after yielding has occurred.

The elastic material parameters are extracted by applying a force that causes a stress well above the yield stress. The resulting curve shows the deflection (h) and applied load (P) at the yield point. From the elastic part of this data the Young's modulus E can be calculated according to [7]:

$$E = \frac{PL^3(1-\nu^2)}{3hI}, \qquad (1)$$

in which L is the effective beam length, ν is Poisson's ratio, and I is the bending moment. The yield stress Y can be calculated from the load at the yield point (P_y) using the following relation [7]:

$$Y = \frac{P_y Lt}{2I}. \qquad (2)$$

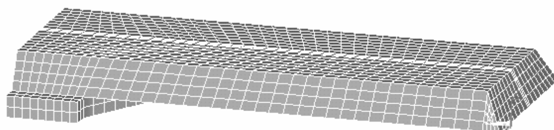

Figure 7: FEM model mesh used to calculate effective length from actual length

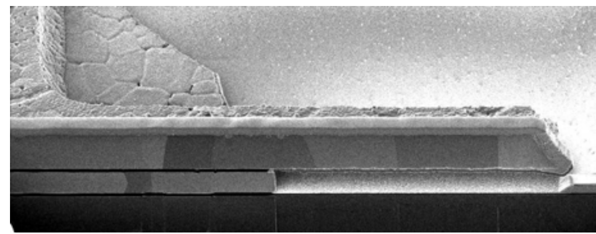

Figure 8: FIB longitudinal cross-sectional image of a micro-beam, showing the columnar grain structure. A deposited line of platinum can be seen along the cutting edge, which is needed in the process.

The presented relations hold for cantilever beams, on which the load is applied at the beam extremity, assuming a perfect fixation and a length-to-thickness ratio of 8:1 [8], which does not fully hold for the test samples used. To correct for this, and to justify the use of equation (1) and (2), an effective length can be used instead of the actual length, such that deviations in geometry, fixation, and load positions are taken into account.

The beam length as used in equation (1) has a third order influence on the extracted Young's modulus. The length used is an effective parameter, based on actual beam length and indenter positioning. A result of this dependency is that errors also play a large role. Two methods are presented to reduce the dependency on the beam length.

The first method obtains the effective length from the actual length by using a continuum-based FEM model. The geometry of the models is created according to the geometry of the test specimens, as can be seen in Figure 7, and the load is positioned at the same position on the beam as the assumed indenter position during the tests. Calculations are carried out using a fixed Young's modulus and load, which give displacement data for the examined cases. The input material properties and load data as well as the resulting deflection is next inserted in equation (1), which then can be altered to obtain the length L. The obtained length L is the effective length of the examined beam, to be used when using equations (1) and (2).

The second method used to eliminate the dependency on the beam length combines equations (1) and (2) under the assumption of a constant Young's modulus, independent on the thickness. This leads to the following expression for the yield stress:

$$Y = \frac{Pt}{2I}\sqrt[3]{\frac{3hIE}{P(1-\nu^2)}} \qquad (3)$$

3. Results

Microstructure

From the OIM measurements a large spread is found on the grain sizes, which is likely to be caused by the absence of temperature control during cooling in the sputtering process.

Authorized licensed use limited to: IEEE Xplore. Downloaded on December 11, 2008 at 01:15 from IEEE Xplore. Restrictions apply.

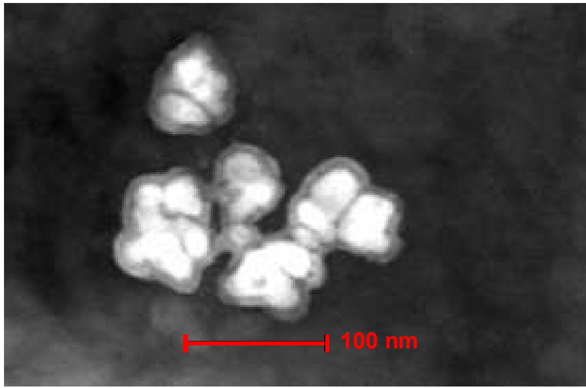

Figure 9: TEM micrograph showing one of the Al_2Cu precipitates. Brightness is a measure for the amount of Cu atoms

The grains are columnar as can be seen in Figure 8, which shows a FIB analysis of the freestanding structure. This image shows a longitudinal cross-section of a cantilever test structure. The average grain diameter in lateral direction equals 5.8 µm with a standard deviation of 3.1 µm. This result is obtained from an OIM measurement on a large area (273 µm x 326 µm). The OIM analysis also shows that the grains have similar orientation, having their {111} plane parallel to the top surface. The orientation of the layer can be explained by the fact that the close packed layer is oriented perpendicularly to the sputter direction, which is the most convenient orientation from an energetic point of view.

The XRD analysis is unable to show Al_2Cu precipitates. The TEM analysis did show precipitates rich in copper, located near the interfaces with SiO_2. Further investigation of these precipitates with EDX showed a 70:30 (at%) Al:Cu ratio, while Al_2Cu has a ratio of 67:33 (at%). For this reason the precipitates are assumed to consist of Al_2Cu. A TEM micrograph showing one of the equilibrium precipitates of type θ is shown in Figure 9. Judging by the size, the type is assumed to be of type θ, an equilibrium Al_2Cu phase.

Table 2: Geometric parameters in µm including standard deviation and number of measurements

Wafer	t_{des} = 3	t_{des} = 4	t_{des} = 5
Length dev. ΔL	+5.42	+4.24	+5.92
sd / no. meas.	0.41 / 20	0.50 / 20	0.59 / 50
Top width w_{top}	23.65	22.18	20.60
sd / no. meas.	0.32 / 20	0.30 / 20	0.41 / 50
Bottom width w_{bot}	25.86	25.00	25.49
sd / no. meas.	0.30 / 20	0.36 / 20	0.58 / 50
Thickness t_{act}	3.06	3.89	4.90
sd / no. meas.	0.05 / 10	0.04 / 10	0.07 / 10

Geometry

The resulting geometry for the different wafers is measured using VSI microscopy. Figure 10 shows how the measured parameters relate to the beam geometry. The results from these measurements are shown in Table 2. The length deviation ΔL expresses the length difference between designed length L_{des} and actual beam length L_{act}, which is measured for a range of beams, including different lengths, hence this presentation. W_{top} and W_{bot} are the top and bottom widths of the beam structures and t_{act} is the layer thickness of the beams as measured. The geometry of the beams has a small spread and the beams present a reproducible geometry.

Bending Experiments

The relation between actual measured beam length L_{act} and effective beam length L_{eff} as obtained from FEM calculations is shown in Figure 11. This relation is used to extract the effective beam length from the measured beam lengths. Using the obtained effective lengths with equation (1) the Young's Modulus is calculated from the measurements, the results of which are shown in Figure 12. The results for the yield stress, using equation (2) with again the obtained effective lengths, are shown in Figure 13.

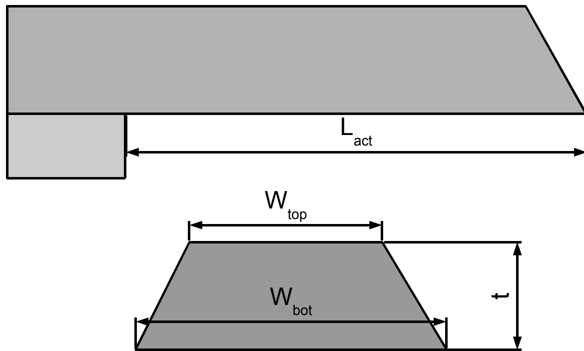

Figure 10: Characteristic size parameters of the microbeams

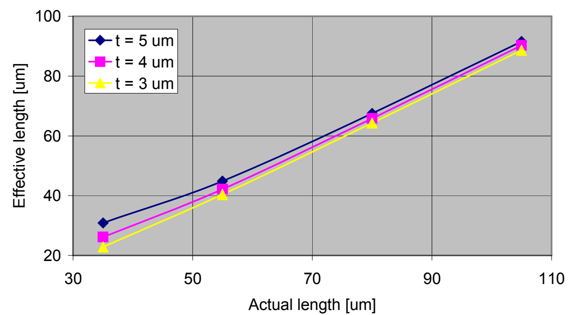

Figure 11: Effective length vs. actual length as calculated using FEM

Authorized licensed use limited to: IEEE Xplore. Downloaded on December 11, 2008 at 01:15 from IEEE Xplore. Restrictions apply.

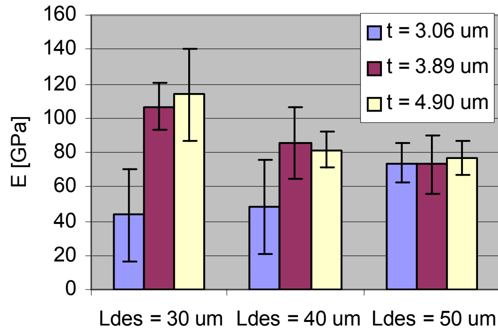

Figure 12: Young's Modulus calculated for L_{des} = 30, 40 & 50 µm and t_{des} = 3, 4 & 5 µm.

The second mentioned method uses Equation (3) to calculate the yield stress. An assumption for the Young's modulus is needed, which is taken as E = 69 GPa, the value of Young's modulus for bulk aluminium. The results of this calculation for the results are shown in Figure 14.

The bending experiment results show a large spread in Young's modulus for small beams. This is likely caused by the error in the effective beam length, which influences the calculated Young's modulus to the third power. The largest beam lengths show smaller spread and are closest to the expected value of E = 69 GPa. A possible explanation is that these beams have the smallest relative length error of the indenter position to the beam length and that the relations used for the calculations are more valid because their length-to-thickness ratio is closer to the value of 8:1, which was assumed in equations (1) and (2).

4. Conclusions & Reccommendations

Due to the large spread in the results no conclusion can be made about the dependence of the Young's modulus on the film thickness for the shorter beams. The longer beams however show no clear dependence on the

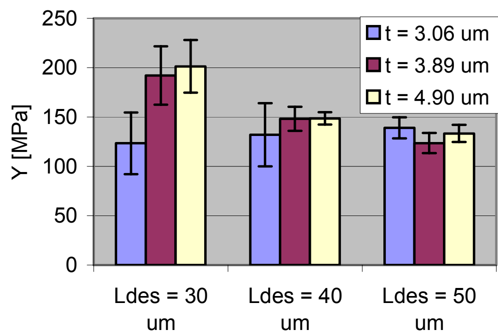

Figure 13: Yield stress calculated for L_{des} = 30, 40 & 50 µm and t_{des} = 3, 4 & 5 µm.

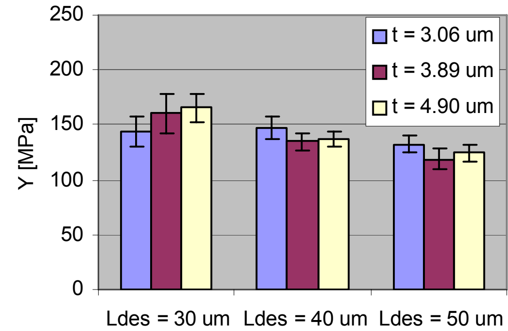

Figure 14: Yield stress calculated assuming E = 69 GPa for L_{des} = 30, 40 & 50 µm and t_{des} = 3, 4 & 5 µm.

film thickness within the measured thickness range, although this effect might still be present.

The yield stress also shows smaller spread for the larger beam lengths, but also no apparent relation to the film thickness is found. The smaller spread in the results for the yield stress compared to the results of the Young's modulus might be explained by the fact that the former is linearly dependent on the beam length, while the latter has a third power dependence on the beam length.

When the yield stress calculation without length dependence is studied, which is shown in Figure 14, a smaller spread is found in the results. This is yet another indication that the beam length is a crucial parameter in this method, but it also shows that other factors, e.g. microstructure and thickness, play an important role as well. As for the yield stress, no clear evidence of a relation between elastic properties and film thickness has been found on the basis of the examined set.

The positioning error of the indenter position is a source of a large error. By using a sharp indenter such as a Berkovich indenter the actual indenter position can be measured afterwards and used as input in the calculations, taking into account the local deformation around the indenter tip.

The use of longer beams is likely to reduce the error made in the effective beam length, since the relative error becomes smaller. This method requires the use of lower forces and improved measurement accuracy.

The use of double-clamped beams in stead of cantilevers might be another option. These beams are less sensitive to positional errors and have higher stiffness, making it possible to use larger loads. The internal stress is not relieved in double-clamped beams and must be measured and included to make accurate calculations.

Even though the results show that the measurement method should be optimised to achieve a better accuracy, the overall conclusion is that the investigated method, possibly making use of the recommended adaptations, holds promise for the mechanical characterization of these freestanding films. Especially in combination with numerical, finite element, simulations, the method is anticipated to give valuable insight in thin film properties

Authorized licensed use limited to: IEEE Xplore. Downloaded on December 11, 2008 at 01:15 from IEEE Xplore. Restrictions apply.

and related size effects. Development of this method is therefore incorporated in our current and future research program.

References

1. Beek, J.T.M. v. et al; “High-Q Integrated RF Passives and RF-MEMS on Silicon,” Mat. Res. Soc. Symp. Proc.Vol. 783, 2004.
2. Nix, William D., “Mechanical Properties of Thin Films,” *Metall. Trans. A,* Vol. 20A (1989) pp. 2217-2245.
3. Arzt, E., “Size Effects in Materials due to Microstructural and Dimensional Constraints: a Comparative Review,” *Acta Mater.* Vol. 46, No 16, (1998) pp. 5611-5626.
4. Landolt, H., & Boernstein, R., Numerical data and functional relationships in science and technology. New Series IV/5, Springer (Berlin), 1998.
5. Callister, William D., Materials Science and Engineering, 5th ed., Wiley (Chichester), 2000.
6. MTS Nano Indenter XP specifications (Jan.2006) http://mtsnano.com/pdf/Nano_IndenterXP.pdf
7. Weihs,T.P., “Mechanical Deflection of Cantilever Microbeams: A New Technique for Testing the Mechanical Properties of Thin Films,” *J. Mater. Res.* Vol. 5, No 3 (1988) pp. 931-942.
8. Roark, Raymond J., *et al*, Formulas for Stress and Strain, 5th ed., McGraw-Hill (London), 1986

Authorized licensed use limited to: IEEE Xplore. Downloaded on December 11, 2008 at 01:15 from IEEE Xplore. Restrictions apply.